EBioMedicine 14 (2016) 83–96

Contents lists available at ScienceDirect

EBioMedicine

journal homepage: www.ebiomedicine.com

Research Paper

Reprogramming macrophage orientation by microRNA 146b targeting transcription factor IRF5

Liang Peng [a], Hui Zhang [a], Yuanyuan Hao [a], Feihong Xu [a], Jianjun Yang [a], Ruihua Zhang [a], Geming Lu [a], Zihan Zheng [a], Miao Cui [a], Chen-Feng Qi [b], Chun Chen [c], Juan Wang [a], Yuan Hu [a], Di Wang [a], Susan Pierce [b], Liwu Li [c], Huabao Xiong [a,d,*]

[a] Department of Medicine, Immunology Institute, Icahn School of Medicine at Mount Sinai,New York, NY 10029, United States
[b] Laboratory of Immunogenetics, National Institute of Allergy and Infectious Diseases, National Institutes of Health, Bethesda, MD 20892, United States
[c] Department of Biological Sciences, Center for Inflammation, Virginia Tech, Blacksburg, VA 24061, United States
[d] Institute of Immunology and Molecular Medicine, Jining Medical College, Jining, Shangdong 272067, China

ARTICLE INFO

Article history:
Received 11 May 2016
Received in revised form 26 October 2016
Accepted 27 October 2016
Available online 29 October 2016

Keywords:
Interleukin 10
miR-146b
Macrophage
CRISPR/Cas9
Colitis

ABSTRACT

The regulation of macrophage orientation pathological conditions is important but still incompletely understood. Here, we show that IL-10 and Rag1 double knockout mice spontaneously develop colitis with dominant M1 macrophage phenotype, suggesting that IL-10 regulates macrophage orientation in inflammation. We demonstrate that IL-10 stimulation induced miR-146b expression, and that the expression of miR-146b was impaired in IL-10 deficient macrophages. Our data show that miR-146b targets IRF5, resulting in the regulation of macrophage activation. Furthermore, miR-146b deficient mice developed intestinal inflammation with enhanced M1 macrophage polarization. Finally, miR-146b mimic treatment significantly suppresses M1 macrophage activation and ameliorates colitis development in vivo. Collectively, the results suggest that IL-10 dependent miR-146b plays an important role in the modulation of M1 macrophage orientation.

1. Introduction

Interleukin 10 (IL-10) is a strong anti-inflammatory cytokine whose role was first reported as IFN-γ suppressing factor acting on Th1 cells (Moore et al., 2001). It has since been shown that IL-10 signals through the IL-10 receptor (IL-10R), which is expressed on a variety of cells, especially many types of immune origin (Moore et al., 2001; Spencer et al., 1998; Tan et al., 1993). The IL-10R complex is composed of two different chains (IL-10R1 and IL-10R2). Binding of IL-10 to the IL-10R activates phosphorylation of the receptor associated Janus tyrosine kinases, resulting in STAT3-mediated signal transduction (Weber-Nordt et al., 1996; Wehinger et al., 1996). IL-10 also inhibit macrophage production of IL-12 (Moore et al., 2001). Recently, we and other groups have demonstrated that IL-10also suppresses Th17 cell differentiation (Franke et al., 2008). IL-10-deficient mice have been shown to spontaneously develop intestinal inflammation characterized by discontinuous transmural lesions affecting intestines, and by dysregulated production of proinflammatory cytokines including IL-12, IL-23, IFN-γ and IL-17(Berg et al., 1995; Kuhn et al., 1993). Several key features of theIL-$10^{-/-}$ chronic intestinal inflammation model are strikingly similar to human inflammatory bowel diseases. Many cell types, including macrophages, produce and respond to IL-10(Moore et al., 2001), but it is currently not understood precisely how IL-10 affects macrophage polarization, or the molecular mechanisms by which IL-10 regulates macrophage gene expressions in the development of inflammatory diseases.

Macrophages are key regulators of both innate and adaptive immunity, serving as essential actors for both inflammatory responses to combat pathogen insult and tissue damage, as well healing responses that help repair affected tissue (Akira et al., 2013; Mills, 2012; Mosser and Edwards, 2008). Macrophages can be differentiated into classically activated macrophages (M1) or alternatively activated macrophages (M2) in response to certain microbial stimuli and/or cytokine signals (Akira et al., 2013; Tugal et al., 2013). M1 macrophages are believed to play an important role in the pathogenesis of various inflammatory diseases (Cassetta et al., 2011; Fernandez-Velasco et al., 2014; Mills, 2012). M1 macrophages produce numerous proinflammatory mediators such as tumor necrosis factor α (TNFα), interleukin-12 and 23, nitric oxide (NO), and other reactive oxygen species (ROS), which are required for host defense against pathogens (Mosser and Edwards, 2008).In contrast, M2 macrophages secrete significant amounts of IL-10 and polyamines, adapting immune responses to promote angiogenesis and tissue remodeling (Biswas and Mantovani, 2010). At the transcriptional level, M1 and M2 macrophages are regulated through different

* Corresponding author at: Immunology Institute, Box 1630, Icahn School of Medicine at Mount Sinai, 1 Gustave L. Levy Place, New York, NY 10029-6574, United States.
E-mail address: Huabao.Xiong@mssm.edu (H. Xiong).

http://dx.doi.org/10.1016/j.ebiom.2016.10.041

mechanisms, with IRF5 serving as a key transcription factor for M1 macrophage differentiation (Lu et al., 2015), while IRF4 is necessary for M2 macrophage differentiation (Krausgruber et al., 2011; Satoh et al., 2010). While recent work has unveiled many of the regulatory targets downstream of these transcription factors, some of the upstream factors that may modulate the expression or activity of these factors remains unknown. In this paper, we explore the role of an IL-10 induced microRNA as a post-transcriptional regulator of IRF5 expression.

MicroRNAs (miRs) are small (22–24 nt) non-coding RNA sequences that primarily function by interacting with the 3′UTRs of gene transcripts and suppressing their translation or driving their degradation (Baumjohann and Ansel, 2013; Friedman et al., 2009; Rebane and Akdis, 2013; Selbach et al., 2008). They are sequentially processed from longer transcripts by the ribo-nuclease III (RNase III) enzymes Drosha and Dicer, after which they exert their function by guiding the Argonaute (AGO) protein-containing miRNA-induced silencing complex (miRISC) to specific target mRNAs through complimentary pairing (Bartel, 2009; Fabian et al., 2010). miRs are integral in regulating gene expression in both innate and adaptive immune cells. Interestingly, recent studies demonstrated that IL-10 regulates the expression of several miRs, including miR187, miR-155, and miR-146a/b (Curtale et al., 2013) (McCoy et al., 2010). For instance, IL-10 can inhibit miR-155 expression induced by TLRs, and promote expression of anti-inflammatory genes (McCoy et al., 2010; O'Connell et al., 2009). Curtale et al. reported that LPS induced expression of miR-146b via an IL-10-dependent loop and showed that miR-146b plays an anti-inflammatory role in human monocytes by direct targeting the TLR4 signaling pathway (Curtale et al., 2013).Despite these studies, the roles played by the IL-10-miRs axis in the control of macrophage orientation and inflammatory disease development remained poorly defined.

In the present study, we show that IL-10 and Rag1 double knockout mice (IL-$10^{-/-}$/$Rag1^{-/-}$) spontaneously develop colitis with high levels of M1 macrophage signature molecules, suggesting that IL-10 regulated M1 macrophages may contribute to the colitis development. We demonstrate that IL-10 or LPS stimulation induced miR-146b expression in macrophages, and that the expression of miR-146b was impaired in IL-10 deficient macrophages. Furthermore, RNA immunoprecipitation assay showed that miR-146b and IRF5 could occupy the same miRNA-induced silencing complex (miRISC). In addition, miR-146b mimic significantly decreased the IRF5 3′UTR activity and IRF5 protein expression induced by LPS. miR-146b deficient mice exhibit enhanced M1 macrophage polarization. Finally, treatment with miR-146b mimic significantly suppressed M1 macrophage activation and ameliorated colitis development. Taken together, the results suggest IL-10-miR-146b-IRF5 axis plays an important role in the modulation of M1 macrophage activation and highlight the role of miR-146b in the control of immune responses.

2. Materials and Methods

2.1. Mice

C57BL/6J (WT), IL-10 deficient, IL-10R2 deficient, and Rag1 deficient mice were obtained from Jackson laboratory and maintained in the barrier facility at the Icahn School of Medicine at Mount Sinai. IL-10/Rag1 double knockout animals were generated by crossbreeding the single knockouts. All animal study protocols were approved by the Institutional Animal Care and Use Committees of Icahn School of Medicine at Mount Sinai.miR-146b deficient mice was generated with CRISP/Cas9 by Applied Stem Cell.

2.2. Preparation of Bone Marrow Derived Macrophages

Bone marrow (BM) cells were isolated from tibias and femurs of C57BL/6 mice following dissection by direct flushing with PBS, and the cells were cultured in the complete DMEM medium supplemented with GM-CSF (10 ng/ml). On day 6 or 7, the resulting bone marrow derived macrophages (BMDMs) were harvested and then seeded in fresh complete DMEM medium at a density of 2×10^6 cells/ml for experiments. Cells further treated with LPS and/or IFN-γ were considered as M1 macrophages.

2.3. Intracellular Staining and Flow Cytometry

Bone marrow derived macrophages were either activated with LPS (100 ng/ml) plus IFN-γ (20 ng/ml) or LPS alone at different concentration overnight, with brefeldin A added to the culture 5 h prior to harvesting. Cells were fixed with IC Fixation Buffer (BD Bioscience), incubated with permeabilization buffer, and consequently stained with PE-anti-mouse IL-12 p40, APC-anti-iNOS and PE-Cy 5.5 anti-mouse CD11b antibodies. For co-culture experiments, CD4, CD44, and CD25 antibodies (all BD biosciences) were also used. Flow cytometry was performed on a FACS (BD Biosciences) and captured data was subsequently analyzed using FlowJo 7.0.

2.4. RNA Isolation and Quantitative Real-time RT–PCR (qPCR)

Total RNA was extracted using an RNeasy plus kit (QIAGEN, Valencia, CA) per the protocol provided, and cDNA was generated with an oligo (dT) primer and the Superscript II system (Invitrogen, USA) followed by analysis using iCycler PCR with SYBR Green PCR master Mix (Applied Biosystems). Results were normalized against the expression of ubiquitin.

2.5. Transfection and Luciferase Reporter Assay

293T cells were transiently transfected with WT or mutant IRF5 3′ UTR luciferase reporter plasmid in the presence of miR-146b mimic at different concentrations. For each transfection, 2.0 μg of plasmid was mixed with 100 μl of DMEM (without additives) and 4.0 μl of Lipofectamine™ 2000 reagent. The mixture was incubated at room temperature for 20 min per the protocol provided and added to 12-well plates containing cells and complete medium. The cells were incubated for 30 h and harvested using reporter lysis buffer (Promega) for determination of luciferase activity. Cells were co-transfected with a β-galactosidase reporter plasmid to normalize experiments for transfection efficiency.

2.6. T cell Proliferation Assay

$CD4^+$ T cells were purified from spleens and lymph nodes of OTII mice and the cells were labeled with CFSE. The labeled cells (1×10^5/well) were co-cultured with macrophages in the absence or presence of anti-CD3 (1 μg/ml) and anti-CD28 (2 μg/ml) antibodies for three days in 96-well microplates. CFSE dilution assay was analyzed using flow cytometry.

2.7. Immunoblotting Analysis

Cells were washed with cold phosphate-buffered saline and lysed for 15 min on ice in 0.5 ml of lysis buffer (50 mM Tris-HCl, pH 8.0, 280 mM NaCl, 0.5% Nonidet P-40, 0.2 mM EDTA, 2 mM EGTA, 10% glycerol, and 1 mM dithiothreitol) containing protease inhibitors. Cell lysates were clarified by centrifugation (4 °C, 15 min, 14,000 rpm) and protein was run on 10% SDS-PAGE gels for immunoblotting. Anti-iNOS (Santa Cruz), anti-IRF5 (MBL), anti-STAT1, and anti-β-actin (Sigma) antibodies were used according to the manufacturer's instructions. Secondary HRP-conjugated antibodies were from Santa Cruz.

2.8. Endotoxin-induced Model of Sepsis

Septic shock in mice was induced by injecting 6 mg/kg *E. coli*-derived ultra-pure LPS or PBS i.p. Survival after injection was monitored and

mice were sacrificed immediately at a humane end point after the observation of a loss of self-righting and insensitivity to touch. A lower-dose model was also applied, in which mice were injected i.p. with LPS (300 μg/mouse) for 4 h and sera were collected as appropriate, along with other key organs such as the spleen.

2.9. Chromatin Immunoprecipitation (ChIP) Assay

ChIP was performed using an assay kit following the manufacturer's instruction (Upstate Biotechnology, Lake Placid NY). Briefly, activated macrophages were cross-linked by exposure to 1% formaldehyde for 10 min at 37 °C.·Nuclei were prepared and subjected to sonication to obtain DNA fragments. Chromatin fractions were precleared with protein A-agarose beads followed by immunoprecipitation overnight at 4 °C with 3 μg of anti-IRF5 (Santa Cruz) or control antibody. Cross-linking was reversed at 65 °C for 4 h, before proteinase K digestion. DNA was purified and subjected to qPCR. The input DNA was diluted 200 times prior to PCR amplification. The input and immunoprecipitated DNA were amplified by qPCR using primers encompassing the known IRF5 binding sites on the IL-12 promoter region.

2.10. Cytokine ELISA

Supernatants from cell cultures were collected after activation under various conditions and secreted cytokines in the supernatants were measured following appropriate dilution by ELISA kits with purified coating and biotinylated detection antibodies: anti-IL-12 p40 (R & D systems), and anti-IL-6, and anti-TNFα (BD Bioscience). All samples were analyzed according to manufacturer instructions.

2.11. Immunoprecipitation of Ago2-bound RNAs (RIP) Assay

Immunoprecipitation of Ago2-bound RNAs, which contains miRs and their target mRNA, was performed as previously described (Curtale et al., 2013). Briefly, 3×10^6 BMDMs derived from C57BL/6 mice were stimulated with LPS (100 ng/ml) plus IFN-γ (20 ng/ml) for 4 h. An aliquot of immunoprecipitation supernatants, corresponding to 0.5×10^6 cell equivalent, was removed after immunoprecipitation as "input". Results were expressed as fold enrichment relative to Ago2-immunoprecipitation control samples.

2.12. IHC and Immunofluorescence

Sections were de-paraffinized in xylene and dehydrated in ethanol. Primary antibody was incubated overnight at 4 °C and secondary biotinylated antibody was detected with streptavidin-HRP or -Fluorescent probe-conjugated antibody. Sections were development using a DAB peroxidase substrate kit (BioGenex). For immunofluorescence, media counting with DAPI was used. Images were acquired using a Nikon Eclipse NE and with NIS elements BR software. Histological score was evaluated as follows (Tomita et al., 2009 #149): submucosa damage, 0; normal or widely scattered leukocytes, 1; focal aggregates of leukocytes, 2; diffuse leukocyte infiltration with expansion of submucosa, 3; diffuse leukocyte infiltration.

2.13. Fluorescence In Situ Hybridization (FISH)

Double digoxin-labeled locked-nucleic acid (LNA) probes (Exiqon) for miR146b were denatured by heating at 90 °C for 4 min then diluted to 40 nM using in situ hybridization buffer (Exiqon). The sections were hybridized with 50 μl of diluted probe at 58 °C for 1 h then washed in decreasing SSC concentrations at hybridization temperature.

2.14. miR-146b Mimic Administration

13-week old IL-$10^{-/-}$ mice were divided into two groups (6 mice/per group): Treatment group and Control group. In the treatment group, IL-$10^{-/-}$ mice were treated with miR-146b mimic intraperitoneally twice a week with 10 mg/kg; while in the control group, mice were treated with miR-146b scramble at same dose for 3 weeks. Body weight was monitored every week and mice were sacrificed 3 weeks later.

2.15. Model Simulation

We constructed a conceptual model consisting of an incoherent feed-forward motif (Fig. S11A) that controls LPS induced M1 macrophage polarization. By using simple hill functions to capture both inhibition and activation relationships between modeling species (IRF5, IL10, miR and IL12 to represent levels of IRF5, IL10, miR146b and IL12 + M1 macrophage population), a set of ordinary differential equations (Eqs. (1)–(4)) was built to describe the rates of changes. We posit that IL12 + M1 macrophage population (IL12) was controlled by IRF5 as evident in Eq. (4). Table S1 lists model parameters, which were adjusted to enable dynamic simulation of observed experimental data. XPPAUT 7.0 (http://www.math.pitt.edu/~bard/xpp/xpp.html) was used to perform the simulation analyses. The .ode file used for simulation is provided in Table S2.

$$\frac{dIRF5}{dt} = g1 \cdot \left(\frac{LPS^{n1}}{km1^{n1} + LPS^{n1}} - \frac{km2^{n2} + k1 \cdot miR^{n2}}{km2^{n2} + miR^{n2}} \cdot IRF5 \right) \quad (1)$$

$$\frac{dIL10}{dt} = g2 \cdot \left(\frac{k2 \cdot LPS^{n3}}{km3^{n3} + LPS^{n3}} - IL10 \right) \quad (2)$$

$$\frac{dmiR}{dt} = g3 \cdot \left(\frac{k3 \cdot IL10^{n4}}{km4^{n4} + IL10^{n4}} - miR \right) \quad (3)$$

$$\frac{dIL12}{dt} = g4 \cdot \left(\frac{IRF5^{n5}}{km5^{n5} + IRF5^{n5}} - IL12 \right) \quad (4)$$

2.16. Statistical Analysis

The results are shown as means ± s.d. and statistical analysis was performed using Student's *t*-test. Where more than two groups were compared, one way-ANOVA with Bonderroni's was performed; Kaplan-Meier was used for survival analysis. P values < 0.05 were considered statistically significant.

3. Results

3.1. IL-10 Regulates M1 Macrophage Polarization During Colitis Development

Although it is well established that IL-10 and IL-10R2 deficient mice spontaneously develop intestinal inflammation, the molecular mechanisms that cause the changes are still not clearly understood. As results, we revisited the development of colitis in IL-10 and IL-10R2 deficient mice. As expected, IL-10 and IL-10R2 deficient mice (13 to 16 weeks of age) spontaneously develop colitis in our animal facility, and histological analysis showed that inflammatory cells were highly infiltrated in the mucosal layers of colons in mice with colitis (Supplementary Fig. 1A). Microarray experiments showed that mRNA expression of M1 macrophage signature genes were significantly increased in intestinal tissues of IL-10 deficient mice with colitis compared with WT mice, and GO analysis showed that the activation of macrophage function was enhanced in IL-$10^{-/-}$ mice (Supplementary Fig. 1B). qPCR experiments

confirm that mRNA expression of iNOS, Il12B, TNFα, and Il6 increased significantly in IL-10 deficient mice (Supplementary Fig. 1C). The levels of IL-12/23p40, TNFα, and IL-6production were significantly increased in IL-10 deficient mice compared with WT mice (Supplementary Fig. 1D). Immunohistological staining indicated that F4/80$^+$iNOS$^+$ cells are clearly present in the mucosa of colon tissues of IL-10 deficient mice (Supplementary Fig. 1E). F4/80$^+$cells and F4/80$^+$ IL-12/23 p40$^+$ cells were present more in the LPMCs of IL-10$^{-/-}$ mice than WT (Supplementary Fig. 1F).

To investigate further the role of IL-10 regulated macrophages in the pathogenesis of colitis, we cross-bred IL-10$^{-/-}$ and Rag1$^{-/-}$ mice and generated IL-10 and Rag1 double knockout mice (IL-10$^{-/-}$/Rag1$^{-/-}$). Interestingly, IL-10$^{-/-}$/Rag1$^{-/-}$ mice spontaneously developed colitis at around 13 weeks of age in our animal facility, as shown by histology and disease score of intestinal inflammation (Fig. 1A, B). qPCR analysis showed that mRNA expression of M1 macrophage signature genes including iNOS, IL-12/23 p40, IL-6, and TNFα significantly increased in intestinal tissues of IL-10$^{-/-}$/Rag1$^{-/-}$ compared with Rag1$^{-/-}$ mice (Fig. 1C). Immunohistological staining showed that iNOS positive F4/80$^+$ cells were present in the mucosa of colons of IL-10$^{-/-}$/Rag1$^{-/-}$ mice (Fig. 1D). IL-12/23p40 and TNFα positive F4/80$^+$ cells were significantly increased in the spleen (data not shown), and MHCII$^+$F4/80$^+$cells were increased in the LPMCs of mucosa of colon in IL-10$^{-/-}$/Rag1$^{-/-}$mice (Fig. 1E, F). Next, we prepared bone marrow-derived macrophages from both Rag1$^{-/-}$ and IL-10$^{-/-}$/Rag1$^{-/-}$ mice and activated the cells with LPS (100 ng/ml) and IFN-γ (20 ng/ml) overnight for M1 macrophage activation and examined the percentage of IL-12p40-producing cells by intracellular staining using flow cytometry. Notably, the frequency of IL-12/23p40-producing cells derived from IL-10$^{-/-}$/Rag1$^{-/-}$ mice was significantly greater than that of cells from Rag1$^{-/-}$ mice (Fig. 1G). Furthermore, the production of TNFα, IL-6 and IL-12/23 p40 was significantly increased in the serum of IL-10$^{-/-}$/Rag1$^{-/-}$ mice (Fig. 1H), suggesting that the increases in cell population had manifest M1 phenotype. Overall, the results suggest that macrophages are strongly skewed towards strong M1 type in IL-10$^{-/-}$/Rag1$^{-/-}$ mice.

3.2. IL-10 Deficiency Enhances M1 Macrophage Polarization

To investigate further the function of IL-10 in macrophage differentiation, we assessed the characteristics of macrophage development in IL-10-deficient mice. Bone marrow cells from IL-10$^{-/-}$ or WT control

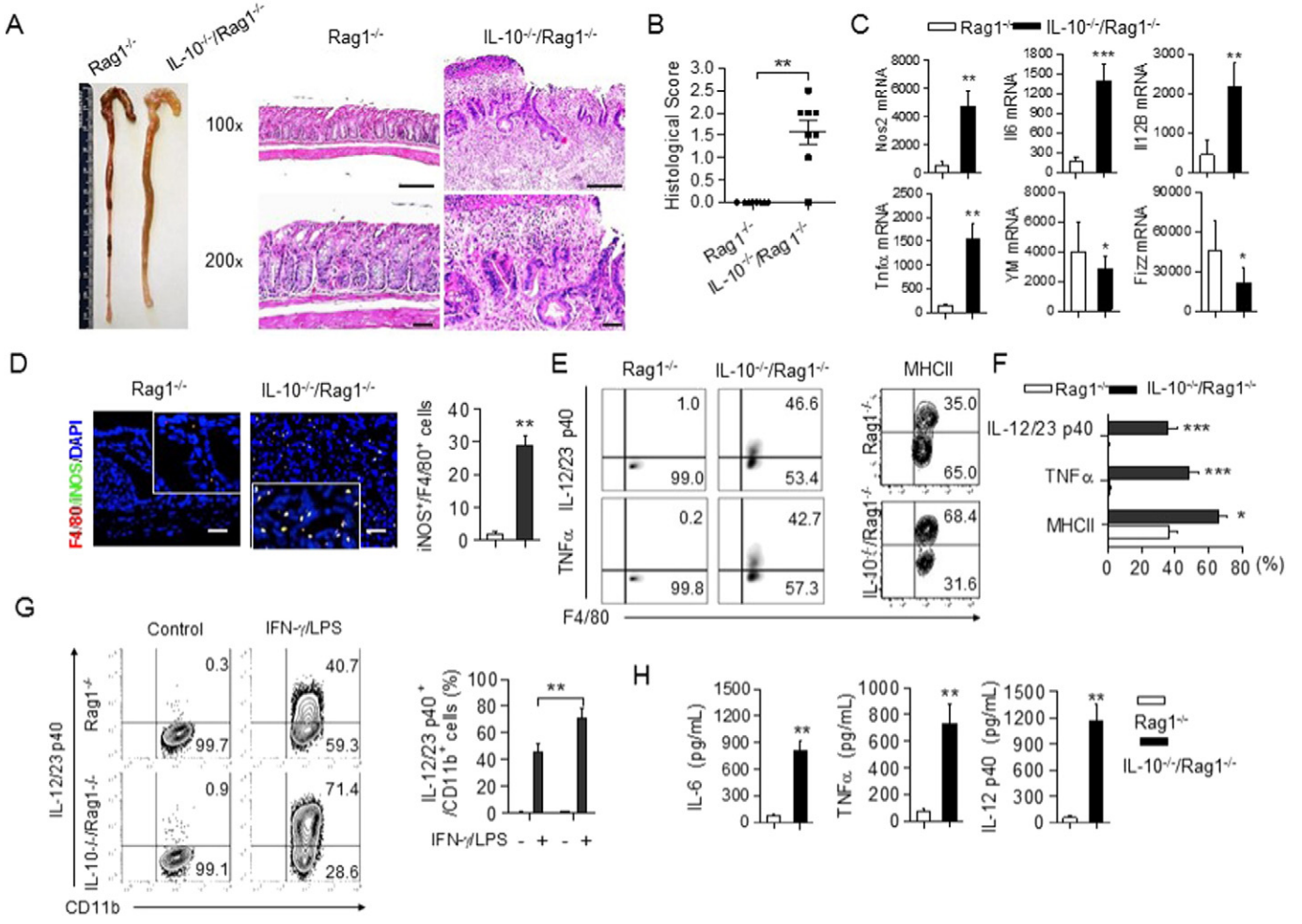

Fig. 1. IL-10 deficient M1 macrophages drive colitis development. Rag$^{-/-}$ and Rag$^{-/-}$/IL-10$^{-/-}$ mice were raised until 20 weeks of age and mice were sacrificed. (A) Photographs of intestinal morphology and H&E staining of colon tissues (upper panel scale bar, 100 μm; low panel scale bar, 50 μm); (B) disease score in the colon tissues of Rag$^{-/-}$ and Rag$^{-/-}$/IL-10$^{-/-}$ mice (*$p < 0.05$). (C) The mRNA levels of TNFα, IL-12/23 p40, and IL-6 in the colon tissue of the WT, IL-10$^{-/-}$ and IL-10R2$^{-/-}$ mice ($n = 5$) (*$p < 0.05$; **$p < 0.01$; ***$p < 0.001$). (D) Detection of iNOS-expressing F4/80 positive cells by immunofluorescence in colon tissue of Rag$^{-/-}$ and Rag$^{-/-}$/IL-10$^{-/-}$ mice (red, F4/80; green, iNOS; blue, DAPI, scale bar, 100 μm). (E, F) The presence of IL-12/23 p40-producing F4/80 positive cells in lamina propria portion of Rag$^{-/-}$ and Rag$^{-/-}$/IL-10$^{-/-}$ mice, with representative FACS dot plots gated on F4/80$^+$ cells and the percentages of IL-12/23 p40-producing cells shown (*$p < 0.05$; **$p < 0.01$; ***$p < 0.001$). (G) BMDMs cultured from Rag$^{-/-}$ and Rag$^{-/-}$/IL-10$^{-/-}$ mice were incubated with IFN-γ (20 ng/ml) plus LPS (100 ng/ml) for 24 h, stained for intracellular IL-12/23 p40, and analyzed by flow cytometry. Representative FACS dot plots gated on CD11b$^+$ cells and the percentage of IL-12/23 p40 positive cells are shown (**$p < 0.01$). (H) ELISA of the serum of the mice detecting the expression of several key pro-inflammatory cytokines, as in (C). All the experiments were repeated three times with similar results.

mice were incubated with GM-CSF (10 ng/ml) in vitro for 7 days. We then performed microarray experiment to examine M1 macrophage signature gene expression at various time points (0, 2, 4, 8 h). As expected, the mRNA expression of all the M1 macrophage signature genes, including IL-6, IL-12B, Nos2, and CXCL2, was significantly increased in IL-$10^{-/-}$ macrophages compared to that of WT cells (Fig. 2A). These results were confirmed via qPCR experiments (Fig. 2B). Flow cytometry analysis showed that the percentages of these M1 signature molecule-expressing cells significantly increased in IL-10 deficient cell cultures compared with WT control cells (Fig. 2C, data now shown).These observations also correlated with the enhanced secretion of IL-12p40, IL-6, and TNFα by IL-$10^{-/-}$ M1 macrophages as determined by ELISA (Fig. 2D). To exclude the possibility that the enhanced M1 macrophage differentiation was due to abnormal myeloid cell development, we examined myeloid cell population from bone marrows and lymph nodes of WT and IL-$10^{-/-}$ mice (Supplementary Fig. 2A), and verified that myeloid cells develop normally in IL-$10^{-/-}$ mice. In addition, we analyzed whether IL-10 signaling cascade affects M1 macrophage differentiation. Similar to IL-10 deficient mice, IL-10R2 deficient mice exhibited enhanced M1 macrophage activation (Supplementary Fig. 2B). The results suggest that IL-10-IL-10R2 signaling cascade plays a negative role in M1 macrophage differentiation.

Since M1 macrophages are known to also be influential on adaptive immune responses, we then sought to investigate how IL-$10^{-/-}$ macrophages regulate T cell activation. We first analyzed expression of MHC II and other co-stimulatory factors in IL-10 deficient macrophages. Bone marrow cells from WT and IL-$10^{-/-}$ mice were activated as before with LPS (100 ng/ml) plus IFN-γ (20 ng/ml) towards M1 macrophage differentiation. The results showed that the percentages of MHC II and CD86 positive cells were significantly higher in IL-10 deficient mice (Supplementary Fig. 3A). Next, we co-cultured WT or IL-$10^{-/-}$ macrophages with OTII $CD4^+$ T cells, and observed that activation markers including CD25 and CD44 were significantly increased in OTII $CD4^+$ T cells co-cultured with IL-$10^{-/-}$ macrophages (Supplementary Fig. 3B). In addition, IFN-γ-producing $CD4^+$ T cells was significantly increased in cultures with IL-10 deficient macrophages (Supplementary Fig. 3C). Taken together, the results indicate that IL-10 deficient macrophages induce stronger T cell activation, consistent with a M1 phenotype.

3.3. miR-146b Induced by IL-10 Suppresses M1 Macrophage Polarization

Since several recent studies have identified that IL-10 can regulate the expression of a few miRs including miR-187, miR-155, miR-146a,

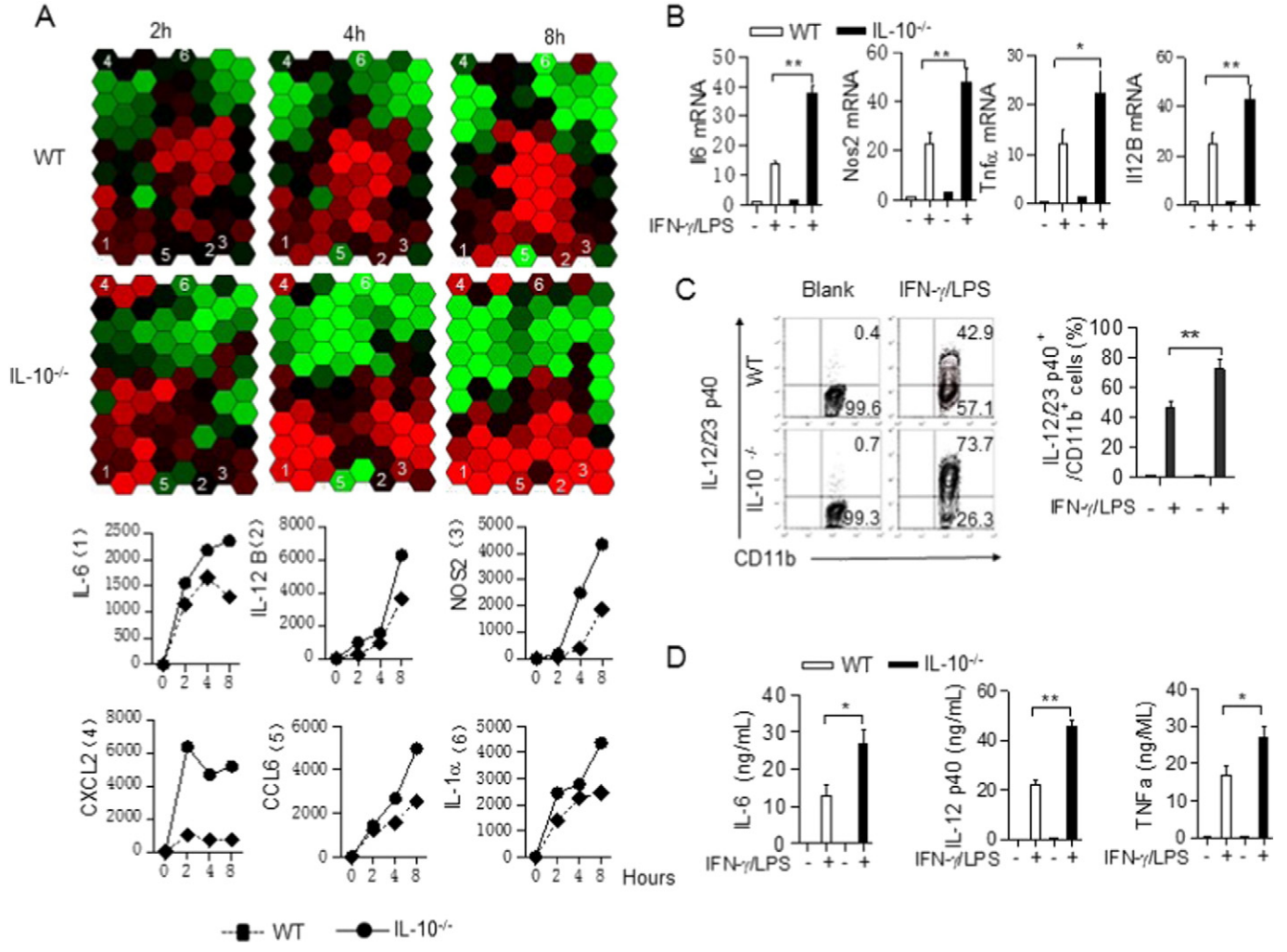

Fig. 2. IL-10 deficiency promotes M1 macrophage differentiation. (A) BMDMs from wild type or IL-$10^{-/-}$ mice were stimulated with IFN-γ (20 ng/ml) plus LPS (100 ng/ml) for various time points (0, 2, 4, 8 h) and mRNA was isolated for microarray analysis. Snapshots from heat maps show 72 genes related to macrophage activation. The position of each gene locus is in the same areas of all six heat maps, with 6 loci of interest being highlighted. (B) BMDMs treated as in (A) for 4 h. Total RNA was prepared and qPCR was performed for the analysis of macrophage gene expression (data represent mean ± s.d.). (C). The cells prepared in A were stimulated with IFN-γ (20 ng/ml) plus LPS (100 ng/ml) overnight and analyzed by flow cytometry. Representative FACS dot plots gated on $CD11b^+$ cells and the percentages of IL-12p/23 p40-producing and iNOS-expressing $CD11b^+$ cells are shown. (D). The cells prepared in (A) were stimulated with IFN-γ (20 ng/ml) plus LPS (100 ng/ml) for 24 h and the supernatants were analyzed for the level of IL-12/23 p40, TNFα and IL-6 production by ELISA. *$p < 0.05$; **$p < 0.01$. The results are representative of three independent experiments.

and miR-146b, we explored the possibility of those miRs contributing to the phenotype observed. To investigate the contribution of miRs exclusively dependent on IL-10 during macrophage polarization, we first analyzed the expression of several previously suggested candidates of interest in WT and IL-10$^{-/-}$ macrophages stimulated with IFN-γ/LPS. The qPCR results showed WT macrophages activated with IFN-γ/LPS did express, miR-155, miR-146a, and miR-146b; however, the expression of miR-146b was the most strikingly impaired in IL-10$^{-/-}$ mice (Supplementary Fig. 4A). The impaired miR-146b expression was confirmed by in situ hybridization (Supplementary Fig. 4B). Thus we focused on miR-146b in the investigation of IL-10 regulation of M1 macrophage polarization. To understand whether miR-146b can affect the M1 macrophage differentiation, bone-marrow-derived macrophages from WT and IL-10$^{-/-}$ mice were transfected with miR-146b mimic. Two days later, the cells were activated with IFN-γ/LPS overnight. The results showed that the percentage of IL-12/23 p40-producing cells was significantly decreased in cultures treated with miR-146b compared with control cultures (Supplementary Fig. 4C). Similarly, the release of cytokines including IL-12 p40, IL-6, and TNFα in the culture supernatants was significantly reduced when analyzed by ELISA (Supplementary Fig. 4D).These results suggest that miR-146b is induced and involved in the activation of M1 macrophages and may modulate M1 macrophage differentiation.

3.4. miR-146b Targets IRF5 in the Regulation of M1 Macrophage Polarization

IRF5 has been defined as a key transcription factor for M1 macrophage differentiation. Bioinformatics analysis revealed that human IRF5 is one of the predicted targets of miR-146b (data not shown).

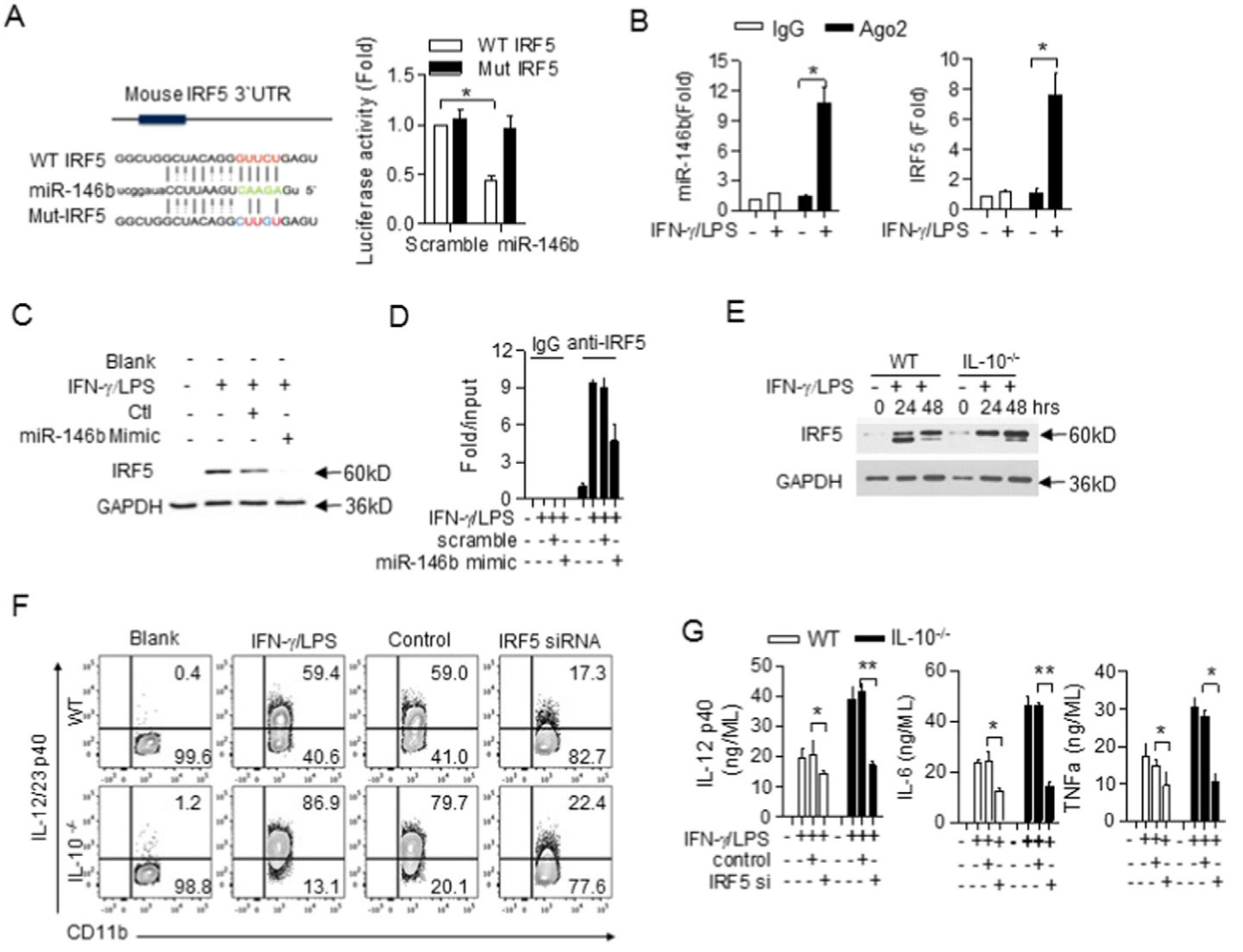

Fig. 3. miR-146b suppresses M1 macrophage activation by targeting IRF5. (A) Schematic representation of wild-type (wt) and mutant (mut) IRF5 3′UTR luciferase reporter constructs. The predicted miR-146b binding region is indicated (left panel). HEK293T cells were co-transfected with either WT or mutant IRF5 luciferase reporter plasmids together the miR-146 mimic for 30 h. The cell lysates were prepared and luciferase activity was detected (Data represent mean ± s.d.). (B) BMDMs from C57BL/6 mice were stimulated with IFN-γ (20 ng/ml) and LPS (100 ng/ml) for 4 h. Total RNA was extracted and immunoprecipitated with anti-Ago2 antibody. The immunoprecipitated RNA was purified and qPCR was performed for the analysis of miR-146b and IRF5 mRNA expression (Data represent mean ± s.d.). (C) BMDMs from C57BL/6 mice were transfected with miR-146b mimic (3 μM) for 48 h and stimulated as in (B) for 24 h. The whole cell lysates were prepared and western blotting was performed for the analysis of IRF5 expression, using GAPDH expression as a control. (D) BMDMs from WT mice were transfected with miR-146b mimic (3 μM) or scramble (3 μM) and stimulated as in B,C for 4 h, followed by ChIP assay. PCR was used to quantify the amount of precipitated DNA with primers flanking the IRF5 binding site in the IL-12 promoter region. (E) Western blot of whole cell lysates from BMDMs of WT and IL-10$^{-/-}$ mice stimulated as before for 24 or 48 h. (F) BMDMs as prepared in A were transfected with either IRF5 siRNA or control siRNA for 48 h and subsequently stimulated as before for 24 h. The cells were stained for intracellular IL-12/23 p40 and analyzed by flow cytometry. Representative FACS dot plots gated on CD11b^{+} cells and the percentage of IL-12/23 p40-producing CD11b^{+} cells is shown. (G) BMDMs prepared in A were transfected with IRF5 siRNA or control siRNA and the cells were then stimulated with IFN-γ (20 ng/ml) and LPS (100 ng/ml) for 24 h. The supernatants were collected and the level of IL-12 p40, TNFα and IL-6 production in the supernatants was analyzed for by ELISA. *$p < 0.05$; **$p < 0.01$. All results are representative of at least two independent experiments.

This putative interaction is conserved between mice and humans (Fig. 3A left).To verify ifmiR-146b really targets IRF5, we constructed luciferase reporter plasmids of the IRF5 3′UTR of mice (including WT and miR-146b binding site mutant copies). The plasmids were then respectively co-transfected with the miR-146b mimic to HEK293T cells. Interestingly, transfection of miR-146b mimic significantly decreased the luciferase activity in cells transfected with IRF5 plasmid; however, miR-146b mimic had no effect on luciferase activity in cells transfected with IRF5 mutant plasmid (Fig. 3A right). RNA immunoprecipitation (RIP) experiments demonstrated that the miR-146b and IRF5 mRNA were in the same miRNA-induced silencing complex (miRISC) (Fig. 3B). This interaction was then evaluated at the protein level, where we found that miR-146b mimic suppressed IRF5 protein expression in IFN-γ/LPS-induced M1 macrophages (Fig. 3C). SinceIRF5 is known to be a key regulator of IL-12 p40, the regulation of IL-12 p40 in the presence ofmiR-146b mimic by ChIP (Fig. 3D). We first examined if IRF5 plays a role in enhanced M1 macrophage differentiation in IL-10$^{-/-}$ mice. Per expectation, IRF5 protein is more stable in IL-10$^{-/-}$ macrophages over time as compared to WT cells (Fig. 3E). Knockdown of IRF5 by siRNA significantly reduced the percentage of IL-12p40-producing cells and cytokine release (Fig. 3F, G).The results indicate that IRF5 is indeed involved in the enhanced M1 macrophage differentiation in IL-10$^{-/-}$ mice. To further confirm that miR-146b targets IRF5 resulting in the regulation of M1 macrophage activation, miR-146b mimic treated macrophages were overexpressed with IRF5 or control plasmid, overexpression of IRF5 rescued miR-146b mimic-induced suppression of M1 macrophage activation and significantly enhanced CD4$^+$ T cell activation (Fig. 4A, B, C, D, E). Thus, the results suggest IL-10-induced miR-146b modulates M1 macrophage differentiation by targeting IRF5.

3.5. miR-146b Deficiency Enhanced M1 Macrophage Orientation

To further analyze the function of miR-146b in the control of macrophage orientation, we generated miR-146b deficient mice by CRISPR/Cas9 (Supplementary Fig. 5A, B, C). Mir146b$^{-/-}$ mice displayed enlarged spleens and increased myeloid cell population and spontaneously developed intestinal inflammation (Fig. 5A, B, C, D; Supplementary Fig. 5D). BMDMs polarized towards M1 inmiR-146b deficient cell cultures showed elevated percentages of IL-12p40$^+$ cells compared with WT controls (Fig. 5E). These observations correlated with enhanced secretion of IL-12p40, IL-6, and TNFα by mir146b$^{-/-}$ M1 macrophages as determined by ELISA (Fig. 5F). In addition, western blot experiments showed that IRF5 protein expression was significantly enhanced inmiR-146b$^{-/-}$ macrophages compared to that of WT cells (Fig. 5G). Furthermore, miR-146b mimic significantly suppressed the expression of M1 macrophage signature genes in Mir146b$^{-/-}$ macrophages (Fig. 5H, I, J). However, IL-10 lost its suppressing effects on M1 macrophage activation in Mir146b$^{-/-}$ macrophages (Fig. 5K, L). These results confirmed that miR-146b is critically involved in M1 macrophage polarization.

Having observed that mir146b$^{-/-}$ macrophages behaved in a manner consistent with an enhanced M1 profile, we then sought to investigate how they regulate T cell activation using co-cultured WT or Mir146b$^{-/-}$ macrophages with OTII CD4$^+$ T cells. The results showed

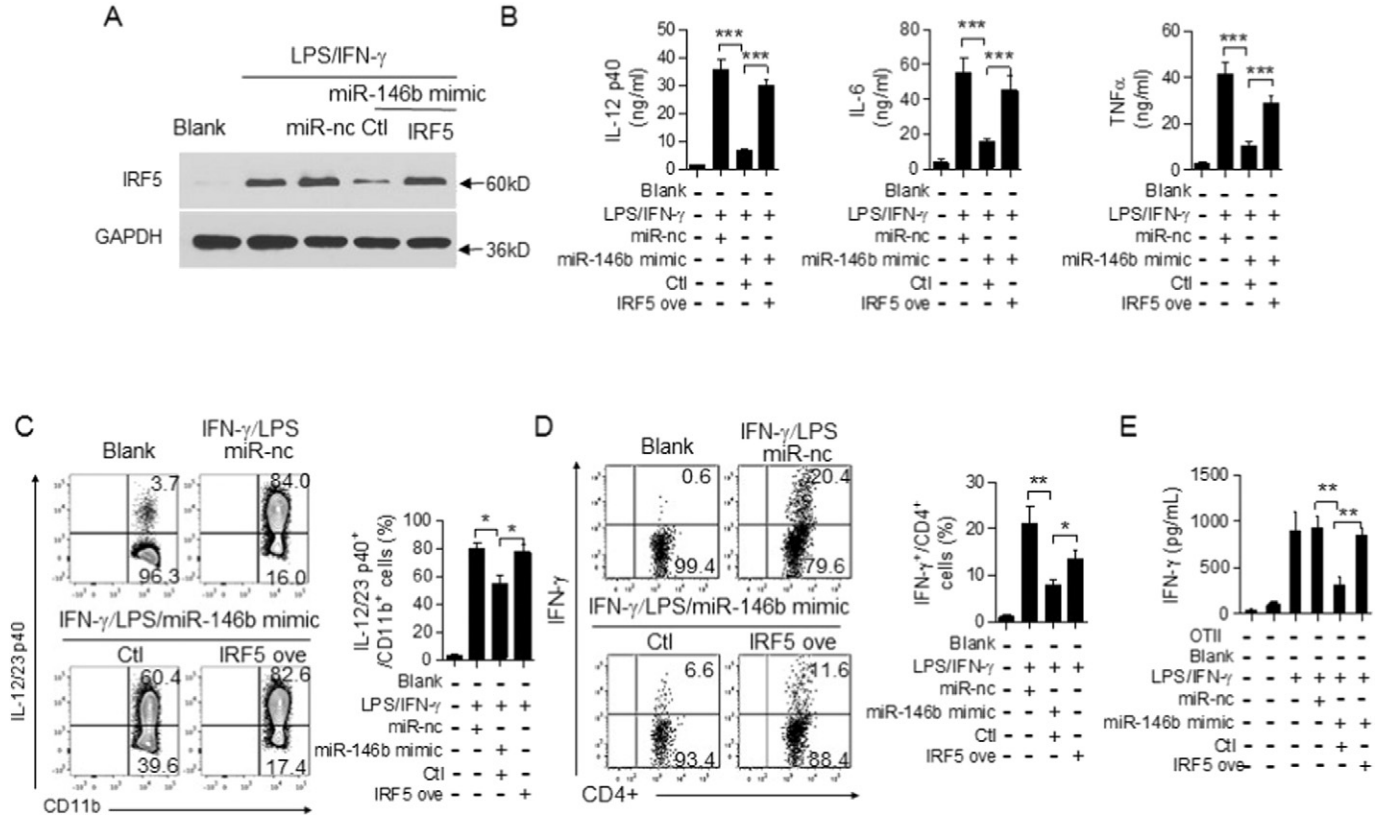

Fig. 4. Overexpression of IRF5 rescued miR-146b mimic-induced suppression of M1 macrophage activation. (A) BMDMs from IL-10$^{-/-}$ mice were transfected with miR-146b mimic (3 μM), miR-nc and IRF5 overexpression plasmid for 48 h and the cells were then stimulated with IFN-γ (20 ng/ml) and LPS (100 ng/ml) for 24 h prior to western blotting for IRF5 expression. (B) BMDMs from C57BL/6 mice were prepared under the same conditions as in A. The supernatants were collected and the level of IL-12 p40, IL-6, and TNFα production in the supernatants was analyzed for by ELISA. ***$p < 0.001$. (C) BMDMs from C57BL/6 mice treated as in B were stained for intracellular IL-12/23 p40 and analyzed by flow cytometry. Representative FACS dot plots gated on CD11b$^+$ cells and the percentage of IL-12/23 p40-producing CD11b$^+$ cells is shown (*$p < 0.05$). (D) CD4$^+$ T cells from spleens and lymph nodes of OTII mice were prepared and the cells were incubated with IL-10$^{-/-}$ BMDMs (unstimulated or stimulated with IFN-γ and LPS) with cotransfection of miR-146b mimic (3 μM), miR-nc and IRF5 overexpression plasmid for three days. The cells were stained for intracellular IFN-γ and analyzed by flow cytometry. Representative FACS dot plots gated on CD4$^+$ cells and the percentages of IFN-γ-producing CD4$^+$ cells are shown. (E) The supernatants in (D) were analyzed for IFN-γ production by ELISA. **$p < 0.01$. All the experiments were repeated three times with similar results.

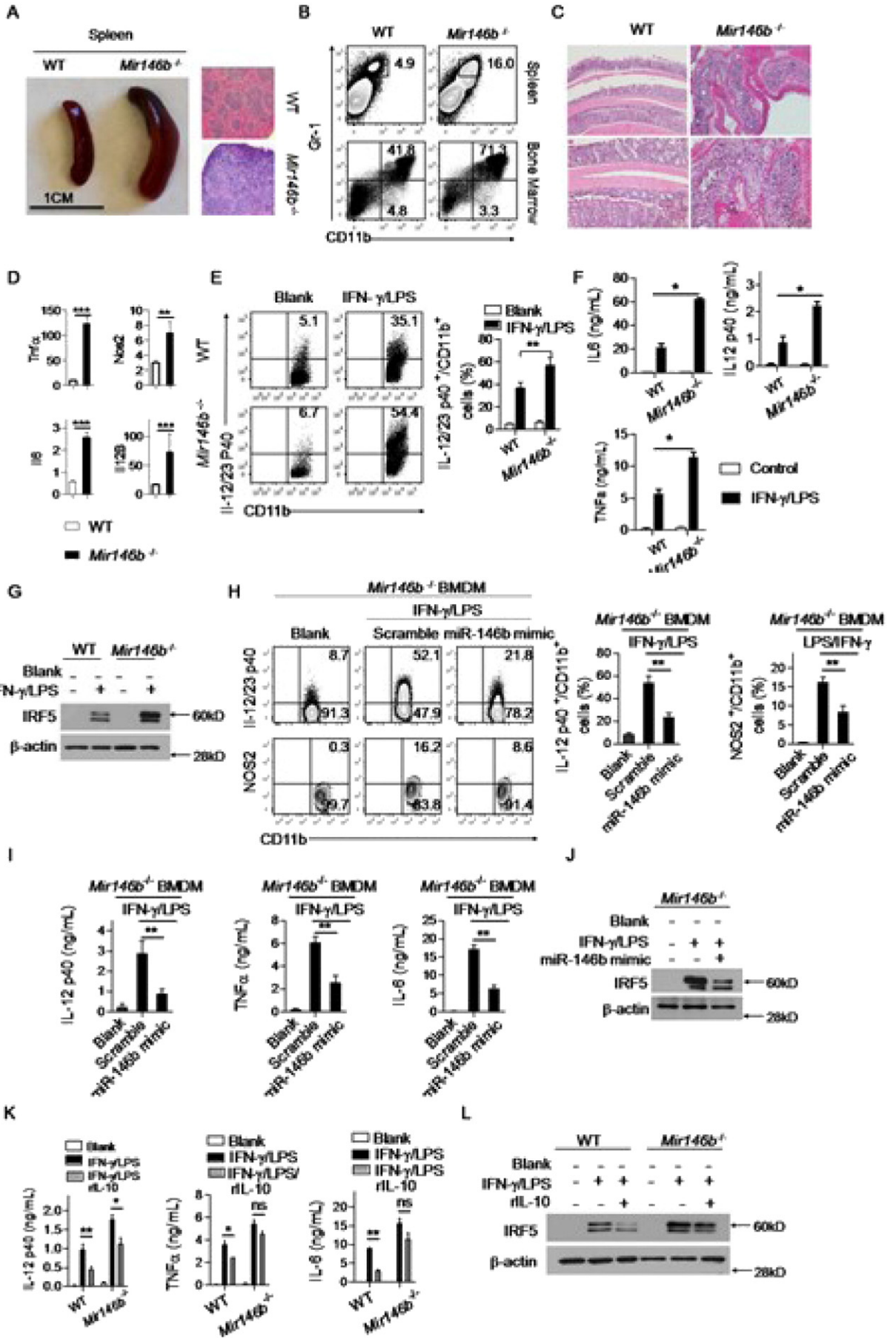
A
Spleen
WT
Mir146b -/-
1CM
B
WT
Mir146b -/-
4.9
16.0
41.8
71.3
4.8
3.3
Spleen
Bone Marrow
Gr-1
CD11b
C
WT
Mir146b -/-
D
Tnfα
Nos2
Il6
Il12b
WT
Mir146b -/-
E
Blank
IFN-γ/LPS
5.1
35.1
6.7
54.4
WT
Mir146b -/-
Il-12/23 P40
CD11b
IL-12/23 p40 +/CD11b+ cells (%)
F
IL6 (ng/mL)
IL12 p40 (ng/mL)
TNFa (ng/mL)
Control
IFN-γ/LPS
G
WT
Mir146b -/-
Blank
IFN-γ/LPS
IRF5
β-actin
60kD
28kD
H
Mir146b -/- BMDM
IFN-γ/LPS
Blank
Scramble miR-146b mimic
8.7
52.1
21.8
91.3
47.9
78.2
0.3
16.2
8.6
99.7
83.8
91.4
Il-12/23 p40
NOS2
CD11b
Mir146b -/- BMDM
IFN-γ/LPS
IL-12 p40 +/CD11b+ cells (%)
Mir146b -/- BMDM
LPS/IFN-γ
NOS2 +/CD11b+ cells (%)
Blank
Scramble
miR-146b mimic
I
Mir146b -/- BMDM
IFN-γ/LPS
IL-12 p40 (ng/mL)
TNFα (ng/mL)
IL-6 (ng/mL)
J
Mir146b -/-
Blank
IFN-γ/LPS
miR-146b mimic
IRF5
β-actin
60kD
28kD
K
Blank
IFN-γ/LPS
IFN-γ/LPS rIL-10
IL-12 p40 (ng/mL)
TNFα (ng/mL)
IL-6 (ng/mL)
WT
Mir146b -/-
L
WT
Mir146b -/-
Blank
IFN-γ/LPS
rIL-10
IRF5
β-actin
60kD
28kD

that activated miR-146b deficient macrophages significantly enhanced $CD4^+$ T cell activation (Fig. 6A, B). CFSE dilution assay showed that there was stronger T cell proliferation in cells co-cultured with $Mir146b^{-/-}$ macrophages compared with WT macrophages (Fig. 6C). However, $Mir146b^{-/-}$ macrophages treated with miR-146b mimic resulted in significantly reduced activation of $CD4^+$ T cell activation (Fig. 6D, E). In addition, $Mir146b^{-/-}$ macrophages were less responsive to IL-10-induced suppression of T cell activation as seen in WT macrophages (Fig. 6F, G). Taken together, the results indicate that miR-146b deficient macrophages induce strong T cell activation.

3.6. Treatment With miR-146b Mimic Ameliorated Colitis Development

Given our results demonstrating the important function of miR-146 in control of gene transcriptional program in M1 macrophage differentiation, we next evaluated potential in vivo effects of miR-146b on M1 macrophage development. First we examined miR-146b expression in intestinal tissues of $IL\text{-}10^{-/-}$ and IL-10R2 mice with colitis. qPCR and in situ experiments showed that miR-146b expression was significantly decreased in the colons of $IL\text{-}10^{-/-}$ mice with colitis compared with WT mice (Fig. 7A, B). These results prompted us to design a miR-146b mimic to test its effectiveness in the control of colitis progress in $IL\text{-}10^{-/-}$ mice. Observations of body weight changed showed no significant changes in mice treated with miR-146b mimic, while mice treated with the scramble continuously lost weight (Fig. 7C). In addition, miR-146b treated mice exhibited improved intestine morphology (Fig. 7D). The disease scores were also significantly lower for miR-146b mimic treated mice compared to their scrambles treated counterparts. And histological study of colon sections from the group mice treated with scrambles further confirmed the presence of more severe inflammatory cell infiltrates, and significantly higher pathological scores than those treated with miR-146b mimic (Fig. 7E,F). qPCR experiments showed that miR-146b expression was significantly increased in the colons of $IL\text{-}10^{-/-}$ mice with mir-146b mimic treatment compared with control (Fig. 7G). Finally, the percentage of IFN-γ or IL-17 positive $CD4^+$ cells significantly decreased in miR-146b mimic treated mice compared with the control mice in the mesenteric lymph nodes and the LPLs (Fig. 7H, Supplementary Fig. 6A). The mice treated with miR-146b had a significantly lower percentage of IL-12 p40- and MHCII expressing macrophages in colon than the scramble-treated mice (Fig. 7I, Supplementary Fig. 6B). In addition, IRF5 expression was decreased in the mucosa of colon with the treatment of miR-146b mimic (Supplementary Fig. 6C). mRNA expression of M1 macrophages signature molecules iNOS, IL-12B, IL-6, and TNFα was significantly reduced in the colons of mice treated with miR-146b mimic compared with control (Supplementary Fig. 6D). Furthermore, IL-12 p40, IL-6, and TNFα was significantly reduced in the serum of mice treated with miR-146b mimic compared with control (Supplementary Fig. 6E). We also tested the effect of miR-146b in an endotoxin shock model. $IL\text{-}10^{-/-}$ mice were injected (i.p.) either with miR-146b mimic or scrambles with 10 mg/kg. 3 h later, mice were then challenged (i.p.) with a lethal dose of LPS (1000 μg/mouse). Susceptibility and the expression of M1 macrophage signature molecules were monitored. The mice treated with miR-146b mimic were more resistant to endotoxin shock (Fig. 8A). The expression and production of M1 macrophage signature molecules including TNFα, IL-12 p40 and others gene were significantly inhibited in mice transferred with the treatment of miR-146b mimic compared with the control; while the expression of M2 macrophage signature genes was increased (Fig. 8B, C). Collectively, these results showed that miR-146b mimic is an effective inhibitor of M1macrophage activation in vivo and ameliorated colitis development in $IL\text{-}10^{-/-}$ mice.

4. Discussion

Interleukin-10 (IL-10) is an important anti-inflammatory cytokine produced by various immune cells and involved in inflammatory diseases. However, the contribution of IL-10 to the polarization of macrophages and molecular mechanisms behind macrophage polarization inflammation are still not fully understood. In the present study, we revisited the IL-10 deficient mice with colitis exhibit enhanced classically activated macrophage phenotype with high expression of IL-12/23 p40, iNOS, TNFα, IL-6, CXCL9, and IRF5. Interestingly IL-10 and Rag1 double knockout mice ($IL\text{-}10^{-/-}/Rag1^{-/-}$) spontaneously develop colitis as well with enhanced expression of M1 macrophage signature molecules. We have shown that IL-10 induces miR-146b expression, which targets IRF5 resulting in the regulation M1 macrophage differentiation (Curtale et al., 2013). MiR-146b deficient mice exhibit enhanced M1 macrophage polarization. Finally, treatment with miR-146b mimic significantly suppressed M1 macrophage polarization in vivo and ameliorated colitis development. Collectively, the results suggest IL-10 expressed in M1 macrophages may play an important role in the reprogramming of M1 macrophage differentiation, resulting in the control of immune responses and pathogenesis of inflammatory diseases.

IL-10 is produced by different cell types including T cells, B cells, mast cells, dendritic cells, and macrophages (Moore et al., 2001). IL-10 has been shown to play an important role in the differentiation and function of Treg cells, and IL-10 secreted from Treg cells has an essential role in maintaining homeostasis in the intestinal mucosa (Veenbergen and Samsom, 2012). Previous studies reported that intestinal macrophages can spontaneously produce IL-10 and these macrophages are believed to be anti-inflammatory, as they actively suppress IL-12 and IL-23 production under non-inflammatory conditions (Murai et al., 2009; Rivollier et al., 2012). In addition, Th17 cells also produce IL-10, resulting in the modulation of inflammatory processes (Zielinski et al., 2012). It is also known that M2 macrophages produce high amount of IL-10, which contributes to the anti-inflammatory functions of M2 macrophages. In the present study, we have demonstrated that IL-10 expressed by M1 macrophages suppresses M1 macrophage activation in inflammation. There are several lines of evidence support this concept. 1). IL-10 and IL-10R2 deficient mice with colitis display an enhanced expression of M1 macrophage signature genes including iNOS, IL-12p40, TNFα, CXCL9, IRF5, etc. 2). The expression of M1 macrophage signature genes is significantly increased in IL-10 and IL-10R2-deficient M1 macrophages. 3). $IL\text{-}10^{-/-}/Rag1^{-/-}$ mice spontaneously develop intestinal inflammation with high expression of M1 macrophage

Fig. 5. miR-146b deficiency enhanced M1 macrophage orientation. WT and $Mir146b^{-/-}$ mice were raised until 12 weeks of age and mice were sacrificed. (A) Photographs of spleen morphology and HE staining. (B) The presence of Gr^+CD11b^+ cells in spleen and Bone marrow cells of WT and $Mir146b^{-/-}$ mice. (C, D) HE staining of colon tissue and qPCR for macrophage genes expression from WT and $Mir146b^{-/-}$ mice. (E) BMDMs from WT and $Mir146b^{-/-}$ were stimulated with IFN-γ (20 ng/ml) and LPS (100 ng/ml) for 24 h, and analyzed by flow cytometry. Representative FACS dot plots gated on $CD11b^+$ cells and the percentage of IL-12/23 p40-producing $CD11b^+$ cells is shown (**$p < 0.01$). (F) The supernatants from (E) were collected and the level of IL-6, IL-12 p40, and TNFα secretion in the supernatants was analyzed by ELISA. *$p < 0.05$. (G) Whole cell lysates of BMDMs from WT and $Mir146b^{-/-}$ were treated as before and analyzed via western blot. (H). BMDMs from $Mir146b^{-/-}$ mice were transfected with miR-146b mimic (3 μM) and miR-nc for 48 h and the cells were then stimulated with IFN-γ (20 ng/ml) and LPS (100 ng/ml) for 24 h. The cells were stained for intracellular IL-12/23 p40, NOS2 and analyzed by flow cytometry. Representative FACS dot plots gated on $CD11b^+$ cells and the percentage of IL-12/23 p40-producing and NOS2-producing $CD11b^+$ cells is shown. (I) The supernatants in (G) were collected and the level of IL-6, IL-12 p40, and TNFα production in the supernatants was analyzed for by ELISA. **$p < 0.01$. (J) The whole cell lysates were prepared and western blotting was performed for the analysis of IRF5 expression after miR146b mimic treatment in $Mir146b^{-/-}$ mice. β-actin expression serves as a control. (K) BMDMs from $Mir146b^{-/-}$ mice were stimulated with IFN-γ (20 ng/ml) and LPS (100 ng/ml) for 24 h in the presence of rIL-10 (10 ng/ml). The supernatants were collected and analyzed for by ELISA. *$p < 0.05$; **$p < 0.01$. (L) The whole cell lysates were prepared and western blotting was performed for the analysis of IRF5 expression. β-actin expression serves as a control. All the experiments were repeated three times with similar results.

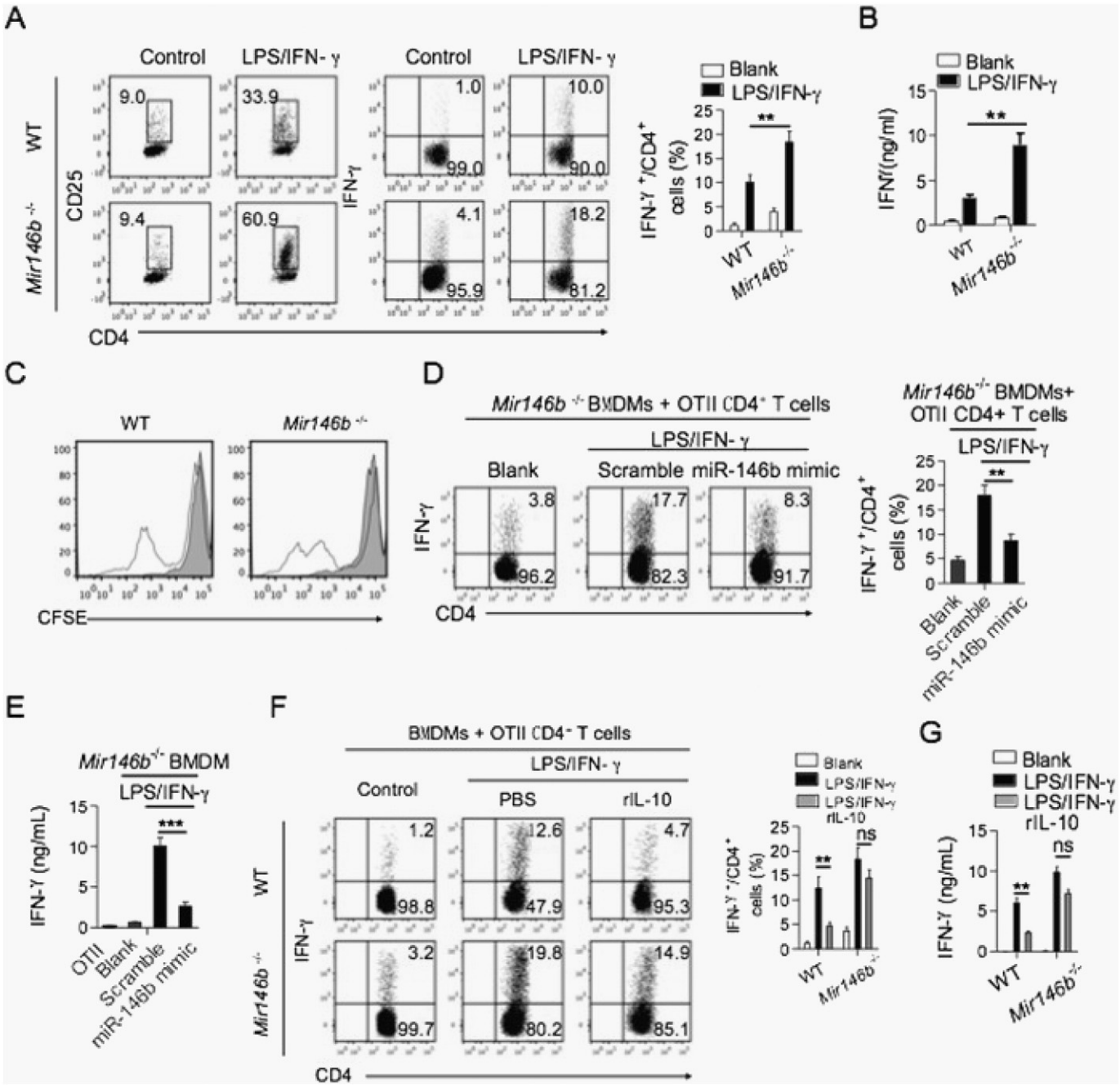

Fig. 6. *Mir146b*$^{-/-}$ macrophages induce enhanced CD4$^+$ T cell activation. (A) CD4$^+$ T cells from spleens and lymph nodes of OTII mice were prepared and the cells were incubated with WT or *Mir146b*$^{-/-}$ BMDMs for three days. Representative FACS dot plots gated on CD4$^+$ cells of the percentages of IFN-γ positive CD4$^+$ cells are shown (**$p < 0.01$). (B) The supernatants were analyzed for IFN-γ production by ELISA (**$p < 0.01$). (C). CD4$^+$ T cells from spleens and lymph nodes of OTII mice were co-cultured as in A and labeled with CFSE. T cell proliferation was analyzed by flow cytometer. (D). CD4$^+$ T cells from spleens and lymph nodes of OTII mice were prepared and the cells were incubated for three days with *Mir146b*$^{-/-}$ BMDMs already transfected with miR-146b mimic. Representative FACS dot plots gated on CD4$^+$ cells and the percentages of IFN-γ positive CD4$^+$ cells are shown. (E) The supernatants were analyzed for IFN-γ production by ELISA. ***$p < 0.001$. (F) CD4$^+$ T cells from spleens and lymph nodes of OTII mice were prepared and the cells were incubated with WT and *Mir146b*$^{-/-}$ BMDMs which were stimulated with IFN-γ (20 ng/ml) and LPS (100 ng/ml) and rIL-10 for 24 h and analyzed as in D. (G) The supernatants were analyzed for IFN-γ production by ELISA. **$p < 0.001$. All the experiments were repeated three times with similar results.

signature genes. Thus, these lines of evidence support the notion that IL-10 expressed in M1 macrophages inhibits M1 macrophage differentiation in inflammation.

IL-10 induces STAT3 activation in myeloid cells resulting in the regulation of proinflammatory gene expression in these cells, and myeloid cell specific deletion of STAT3 develop colitis in a phenomena similar to IL-10 deficient mice (Kobayashi et al., 2003), suggesting that STAT3 is key immediate of IL-10 signaling cascade. Interestingly, colitis developed in myeloid-specific STAT3 KO mice can be prevented by TLR4 deficiency (Kobayashi et al., 2003). In addition, MyD88 deficiency completely rescues colitis in IL-10 deficient mice (Rakoff-Nahoum et al., 2006). Recently, Hoshi et al. reported that MyD88 signaling in colonic mononuclear phagocytes drives colitis development in IL-10 deficient mice (Hoshi et al., 2012). They demonstrated that Villin-MyD88/IL-10 KO mice developed colitis comparable to IL-10 deficient mice. However, CD11c-MyD88/IL-10 or LysM-MyD88/IL-10 KO mice showed minimal signs of intestinal inflammation. Furthermore, recent reports suggest IL-10-IL-10R signaling cascade restricted to macrophage is important for colitis development (Shouval et al., 2014; Zigmond et al., 2014). Taken together, these observations suggest that IL-10 induced by TLR-

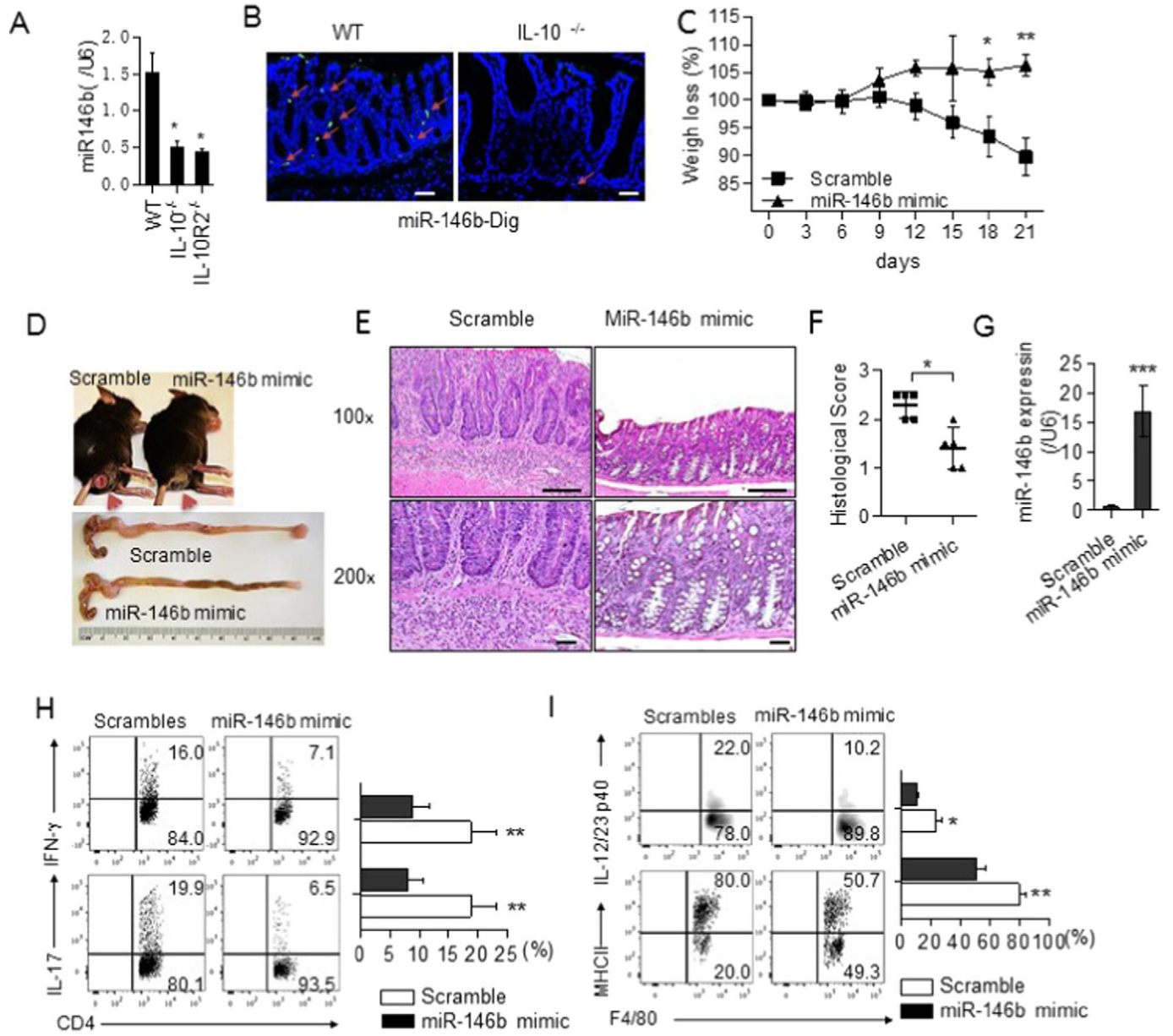

Fig. 7. Treatment with miR-146b mimic suppressed M1 macrophage activation in vivo and ameliorated colitis development. 16-week old WT, IL-$10^{-/-}$, and IL-10R2$^{-/-}$ mice were sacrificed and colons were removed. (A) Total RNA was extracted from colon tissues and qPCR was performed for the expression of miR-146b. (B) In situ hybridization was performed for the detection of miR-146b expression in colon tissues in WT and IL-$10^{-/-}$ mice. The data are representative of two independent experiments. (C) 13-week old IL-$10^{-/-}$ mice were divided into two groups (6 mice/per group). In the treatment group, IL-$10^{-/-}$ mice were treated with miR-146b mimic intraperitoneally twice a week at 10 mg/kg; while in the control group, mice were treated with miR-146b scramble at same dose for 3 weeks. Body weight was monitored every week and mice were sacrificed 3 weeks later. Changes in body weight of IL-$10^{-/-}$ mice (n = 5 mice per group) treated either with miR146b scramble or mimic were recorded. Data are presented as the mean ± s.d. of the percentage of initial body weight. (D) Morphology of intestines, (E) sections of colons with colitis, (F) disease scores from IL-$10^{-/-}$ mice three weeks after treated either with 146b mimic or scramble (n = 5 mice in each group). *$p < 0.05$. (G) miR146b expression in colon of the scramble and miR146b mimic treatment group (***$p < 0.001$). (H) The percentages of IL-17- or IFN-γ-producing cells from intestinal lamina propria lymphocytes of IL-$10^{-/-}$ mice (**$p < 0.01$). (I) The percentages of IL-12/23 p40-producing and MHCII-expressing cells from intestinal lamina propria cells of IL-$10^{-/-}$ mice. Representative FACS dot plots gated on F4/80^{+} cells and the percentage of IL-12/23 p40-producing and MHCII-expressing cells are shown (n = 6), (*$p < 0.05$; **$p < 0.01$).

MyD88 signaling pathways is essential for the control of colitis development.

It is well-known that IL-10 can suppress proinflammatory cytokine gene expressions from different cell types including T cells and macrophages; however, the molecular mechanisms for the inhibitory effects of IL-10 have not been fully defined. Previously, Zhou et al. reported that IL-10 abolished recruitment of RNA polymerase II to the IL-12/23 p40 promoter in LPS-stimulated macrophages resulted in the suppressing of IL-12/23 p40 gene transcription (Zhou et al., 2004). Driessler et al. demonstrated that IL-10 selectively induced nuclear translocation and DNA-binding of the repressive NF-κB p50/p50 homodimer is an important mechanism for IL-10 to repress inflammatory gene transcription (Driessler et al., 2004). Kabayashi et al. found that acetylated histone H4 transiently associated with the IL-12/23 p40 promoter in WT macrophages, whereas association of these factors was prolonged in IL-10 deficient macrophages (Kobayashi et al., 2012). In addition, experiments using histone deacetylase inhibitors and HDAC3 short hairpin RNA indicates that HDACs are involved in histone deacetylation of the IL-12/23 p40 promoter by IL-10(Kobayashi et al., 2012). They suggest that histone acetylation on IL-12/23 p40 promoter by HDAC3 mediates

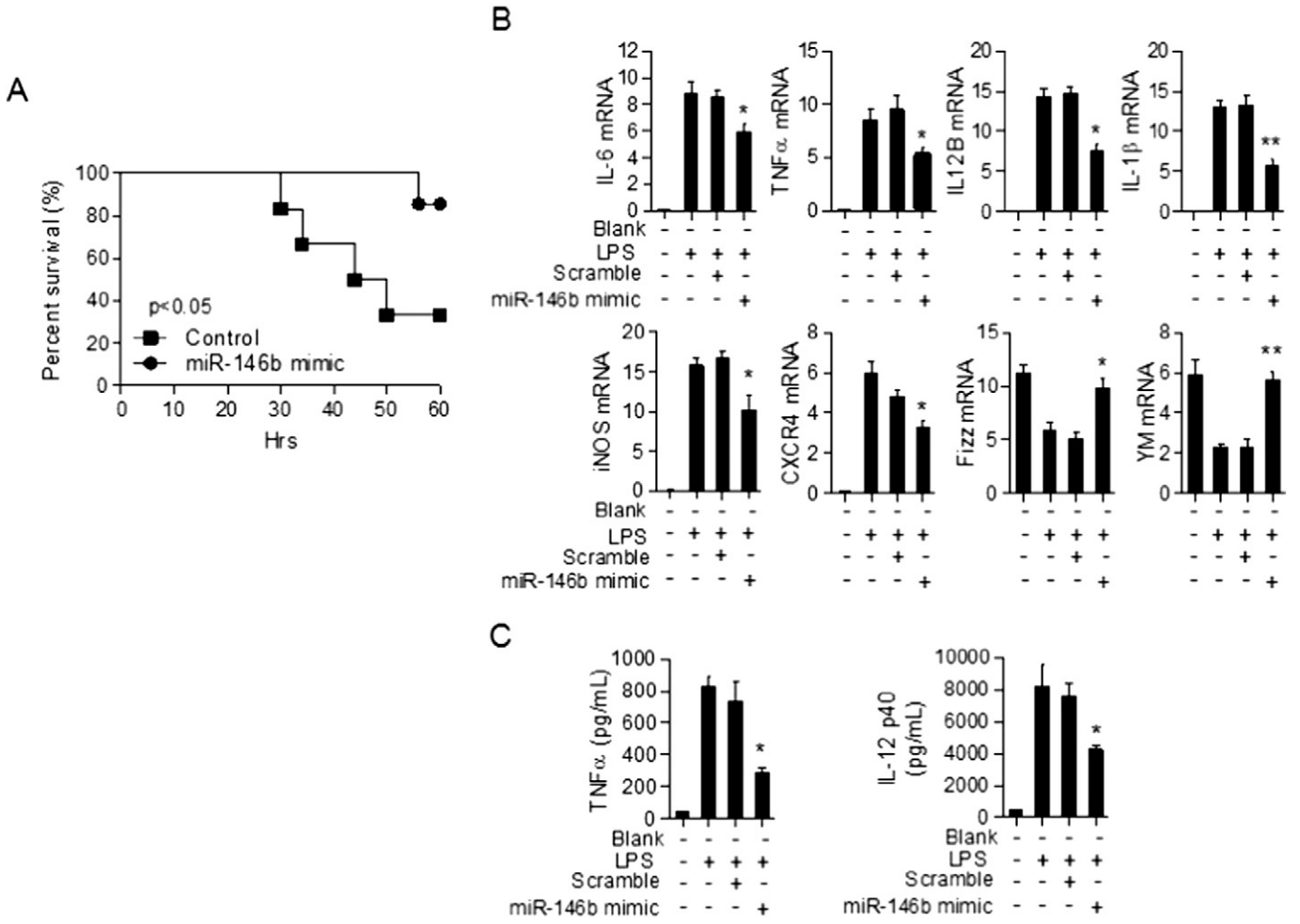

Fig. 8. miR-146b mimic ameliorates endotoxin shock in mice. 7 week old IL-10$^{-/-}$ mice were divided into two group (n = 10/per group) and one group of mice were injected (i.p.) with miR-146b scramble and the other group of mice were injected (i.p.) with miR-146b mimic at a dose of 10 mg/kg. (A) 3 h later both groups of mice were challenged (i.p.) with LPS (1000 μg/per mouse) and the survival of mice was monitored. (B, C) 3 h later both groups of mice were challenged (i.p.) with LPS (300 μg/per mouse) and mice were sacrificed 4 h later. Total RNA was extracted from the spleens of mice and qPCR was performed for the analysis of M1 and M2 macrophage signature gene expression. The sera level of IL-6 and TNFα was determined by ELISA. *$p < 0.05$, **$p < 0.01$.The results were representative of two independent experiments.

homeostatic effects of IL-10 in macrophages. Taken together, these observations indicate that IL-10 may act through diverse mechanisms in the suppression of proinflammatory gene expressions.

Recently, it has been demonstrated that IL-10 can regulate miR expressions resulting in the anti-inflammatory functions. McCoy et al. have shown that IL-10 suppressed the expression of miR-155 induced by TLR activation, enhancing the expression of the miR-155 target gene SH2 domain-containing inositol-5-phosphatase 1 (SHIP1) (McCoy et al., 2010). In addition, Curtale et al. have demonstrated that LPS induces expression of miR-146b via an IL-10-dependent and miR-146b modulated the TLR4 signaling pathway by direct targeting of multiple elements, including TLR4, MyD88, IRAK1, and TRAF6 (Curtale et al., 2013). The enforced expression of miR-146b in human monocytes leads to a significant reduction in the LPS-dependent production of proinflammatory cytokines and chemokines (Curtale et al., 2013). In the present study, we found that miR-146b was induced in murine M1 macrophages after stimulation with LPS and miR-146b expression was impaired in IL-10 deficient cells. Importantly, we demonstrated that enforced expression of miR-146b significantly suppressed M1 macrophage differentiation by suppressing M1 macrophage signature gene expression. In addition, we identified that the miR-146b targets IRF5, a key transcription factor for M1 macrophage differentiation. Furthermore, miR-146b deficient mice exhibit enhanced M1 macrophage polarization. Thus it may be concluded that IL-10 induces the expression of miR-146b, which targets IRF5 in the modulation of M1 macrophage differentiation.

Our mechanistic studies reveal a key dynamic process that underlies the modulation of macrophage polarization. As summarized in the Supplementary Fig. 8, our experimental study derives a key time-delayed incoherent feed-forward control mechanism responsible for the transient nature of M1 macrophage polarization by LPS. The initial pro-inflammatory M1 response to LPS may be due to the rapid activation of IRF5. The subsequent induction of IL-10, followed by the expression of miR-146b sets in motion a time-delayed negative attenuation of IRF5. This delayed negative motif eventually attenuates M1 polarization. By distilling this key dynamic motif, we have constructed a skeletal computational model to re-capture this transient dynamics in macrophage differentiation (Supplementary Fig. 7).

Several techniques have been set up to explore the therapeutic potential of miRs. miRs can be deactivated and silenced by anti-miR oligonucleotides (AMOs), “miR sponges”, and “miR masking” (McDermott et al., 2011). Conversely, other treatments simply restore their expression. This can be achieved through miR mimic or plasmid/viral vector-encoded miR replacement. miR mimics are small chemically altered double stranded RNA molecules that imitate endogenous miRs (McDermott et al., 2011). Plasmid/viral vectors encoding miRs are encouraging strategies to replace miRs in vivo, with good transduction efficiency and minimal toxicity (Brown et al., 2006; Colin et al., 2009).

Therefore, the development of miR-based therapeutics is of great interest in various diseases (Banno et al., 2014; Boon et al., 2013; Ge et al., 2014; Kornfeld et al., 2013; Sun et al., 2012). In the present study, we found that miR-146b expression was significantly decreased in IL-10 deficient mice with colitis, which prompted us to test miR-146b mimic in the treatment of colitis in IL-$10^{-/-}$ mice. Interestingly, compared with scrambles, treatment with miR-146b mimic is effective in amelioration of colitis in IL-$10^{-/-}$ mice maybe through suppressing M1 macrophage differentiation. The results will suggest targeting miR-146b can control M1 macrophage activation and ameliorate colitis development.

Thus, our studies demonstrate that IL-10 dependent miR-146b expressed in M1 macrophages modulates shaping of macrophage phenotype. We suggest a novel mechanism for the effect of miR-146b targeting IRF5 in the modulation of M1 macrophage differentiation. Treatment with miR-146b mimic significantly improved colitis development and clearly suppressed M1 macrophage activation by inhibiting the expression of M1 macrophage signature genes in vitro and in vivo. Taken together, the results firmly establish IL-10 dependent miR-146b plays an important role in the modulation of M1 macrophage activation and highlight the potent role of miR-146b in the control of immune responses and pathogenesis of inflammatory diseases.

Competing Interest Statement

The authors declare that they have no competing interests.

Acknowledgement

H.X. was supported by the NIH funding (RO1AI104688).

Appendix A. Supplementary Data

Supplementary data to this article can be found online at http://dx.doi.org/10.1016/j.ebiom.2016.10.041.

References

Akira, S., Misawa, T., Satoh, T., Saitoh, T., 2013. Macrophages control innate inflammation. Diabetes Obes. Metab. 15 (Suppl. 3), 10–18.

Banno, K., Yanokura, M., Iida, M., Adachi, M., Nakamura, K., Nogami, Y., Umene, K., Masuda, K., Kisu, I., Nomura, H., et al., 2014. Application of MicroRNA in diagnosis and treatment of ovarian cancer. Biomed. Res. Int. 2014, 232817.

Bartel, D.P., 2009. MicroRNAs: target recognition and regulatory functions. Cell 136, 215–233.

Baumjohann, D., Ansel, K.M., 2013. MicroRNA-mediated regulation of T helper cell differentiation and plasticity. Nat. Rev. Immunol. 13, 666–678.

Berg, D.J., Leach, M.W., Kuhn, R., Rajewsky, K., Muller, W., Davidson, N.J., Rennick, D., 1995. Interleukin 10 but not interleukin 4 is a natural suppressant of cutaneous inflammatory responses. J. Exp. Med. 182, 99–108.

Biswas, S.K., Mantovani, A., 2010. Macrophage plasticity and interaction with lymphocyte subsets: cancer as a paradigm. Nat. Immunol. 11, 889–896.

Boon, R.A., Iekushi, K., Lechner, S., Seeger, T., Fischer, A., Heydt, S., Kaluza, D., Treguer, K., Carmona, G., Bonauer, A., et al., 2013. MicroRNA-34a regulates cardiac ageing and function. Nature 495, 107–110.

Brown, B.D., Venneri, M.A., Zingale, A., Sergi Sergi, L., Naldini, L., 2006. Endogenous microRNA regulation suppresses transgene expression in hematopoietic lineages and enables stable gene transfer. Nat. Med. 12, 585–591.

Cassetta, L., Cassol, E., Poli, G., 2011. Macrophage polarization in health and disease. ScientificWorldJournal 11, 2391–2402.

Colin, A., Faideau, M., Dufour, N., Auregan, G., Hassig, R., Andrieu, T., Brouillet, E., Hantraye, P., Bonvento, G., Deglon, N., 2009. Engineered lentiviral vector targeting astrocytes in vivo. Glia 57, 667–679.

Curtale, G., Mirolo, M., Renzi, T.A., Rossato, M., Bazzoni, F., Locati, M., 2013. Negative regulation of Toll-like receptor 4 signaling by IL-10-dependent microRNA-146b. Proc. Natl. Acad. Sci. U. S. A. 110, 11499–11504.

Driessler, F., Venstrom, K., Sabat, R., Asadullah, K., Schottelius, A.J., 2004. Molecular mechanisms of interleukin-10-mediated inhibition of NF-kappaB activity: a role for p50. Clin. Exp. Immunol. 135, 64–73.

Fabian, M.R., Sonenberg, N., Filipowicz, W., 2010. Regulation of mRNA translation and stability by microRNAs. Annu. Rev. Biochem. 79, 351–379.

Fernandez-Velasco, M., Gonzalez-Ramos, S., Bosca, L., 2014. Involvement of monocytes/macrophages as key factors in the development and progression of cardiovascular diseases. Biochem. J. 458, 187–193.

Franke, A., Balschun, T., Karlsen, T.H., Sventoraityte, J., Nikolaus, S., Mayr, G., Domingues, F.S., Albrecht, M., Nothnagel, M., Ellinghaus, D., et al., 2008. Sequence variants in IL10, ARPC2 and multiple other loci contribute to ulcerative colitis susceptibility. Nat. Genet. 40, 1319–1323.

Friedman, R.C., Farh, K.K., Burge, C.B., Bartel, D.P., 2009. Most mammalian mRNAs are conserved targets of microRNAs. Genome Res. 19, 92–105.

Ge, Q., Brichard, S., Yi, X., Li, Q., 2014. microRNAs as a new mechanism regulating adipose tissue inflammation in obesity and as a novel therapeutic strategy in the metabolic syndrome. J. Immunol. Res. 2014, 987285.

Hoshi, N., Schenten, D., Nish, S.A., Walther, Z., Gagliani, N., Flavell, R.A., Reizis, B., Shen, Z., Fox, J.G., Iwasaki, A., et al., 2012. MyD88 signalling in colonic mononuclear phagocytes drives colitis in IL-10-deficient mice. Nat. Commun. 3, 1120.

Kobayashi, M., Kweon, M.N., Kuwata, H., Schreiber, R.D., Kiyono, H., Takeda, K., Akira, S., 2003. Toll-like receptor-dependent production of IL-12p40 causes chronic enterocolitis in myeloid cell-specific Stat3-deficient mice. J. Clin. Invest. 111, 1297–1308.

Kobayashi, T., Matsuoka, K., Sheikh, S.Z., Russo, S.M., Mishima, Y., Collins, C., deZoeten, E.F., Karp, C.L., Ting, J.P., Sartor, R.B., et al., 2012. IL-10 regulates Il12b expression via histone deacetylation: implications for intestinal macrophage homeostasis. J. Immunol. 189, 1792–1799.

Kornfeld, J.W., Baitzel, C., Konner, A.C., Nicholls, H.T., Vogt, M.C., Herrmanns, K., Scheja, L., Haumaitre, C., Wolf, A.M., Knippschild, U., et al., 2013. Obesity-induced overexpression of miR-802 impairs glucose metabolism through silencing of Hnf1b. Nature 494, 111–115.

Krausgruber, T., Blazek, K., Smallie, T., Alzabin, S., Lockstone, H., Sahgal, N., Hussell, T., Feldmann, M., Udalova, I.A., 2011. IRF5 promotes inflammatory macrophage polarization and TH1-TH17 responses. Nat. Immunol. 12, 231–238.

Kuhn, R., Lohler, J., Rennick, D., Rajewsky, K., Muller, W., 1993. Interleukin-10-deficient mice develop chronic enterocolitis. Cell 75, 263–274.

Lu, G., Zhang, R., Geng, S., Peng, L., Jayaraman, P., Chen, C., Xu, F., Yang, J., Li, Q., Zheng, H., et al., 2015. Myeloid cell-derived inducible nitric oxide synthase suppresses M1 macrophage polarization. Nat. Commun. 6, 6676.

McCoy, C.E., Sheedy, F.J., Qualls, J.E., Doyle, S.L., Quinn, S.R., Murray, P.J., O'Neill, L.A., 2010. IL-10 inhibits miR-155 induction by toll-like receptors. J. Biol. Chem. 285, 20492–20498.

McDermott, A.M., Heneghan, H.M., Miller, N., Kerin, M.J., 2011. The therapeutic potential of microRNAs: disease modulators and drug targets. Pharm. Res. 28, 3016–3029.

Mills, C.D., 2012. M1 and M2 macrophages: oracles of health and disease. Crit. Rev. Immunol. 32, 463–488.

Moore, K.W., de Waal Malefyt, R., Coffman, R.L., O'Garra, A., 2001. Interleukin-10 and the interleukin-10 receptor. Annu. Rev. Immunol. 19, 683–765.

Mosser, D.M., Edwards, J.P., 2008. Exploring the full spectrum of macrophage activation. Nat. Rev. Immunol. 8, 958–969.

Murai, M., Turovskaya, O., Kim, G., Madan, R., Karp, C.L., Cheroutre, H., Kronenberg, M., 2009. Interleukin 10 acts on regulatory T cells to maintain expression of the transcription factor Foxp3 and suppressive function in mice with colitis. Nat. Immunol. 10, 1178–1184.

O'Connell, R.M., Chaudhuri, A.A., Rao, D.S., Baltimore, D., 2009. Inositol phosphatase SHIP1 is a primary target of miR-155. Proc. Natl. Acad. Sci. U. S. A. 106, 7113–7118.

Rakoff-Nahoum, S., Hao, L., Medzhitov, R., 2006. Role of toll-like receptors in spontaneous commensal-dependent colitis. Immunity 25, 319–329.

Rebane, A., Akdis, C.A., 2013. MicroRNAs: essential players in the regulation of inflammation. J. Allergy Clin. Immunol. 132, 15–26.

Rivollier, A., He, J., Kole, A., Valatas, V., Kelsall, B.L., 2012. Inflammation switches the differentiation program of Ly6Chi monocytes from antiinflammatory macrophages to inflammatory dendritic cells in the colon. J. Exp. Med. 209, 139–155.

Satoh, T., Takeuchi, O., Vandenbon, A., Yasuda, K., Tanaka, Y., Kumagai, Y., Miyake, T., Matsushita, K., Okazaki, T., Saitoh, T., et al., 2010. The Jmjd3-Irf4 axis regulates M2 macrophage polarization and host responses against helminth infection. Nat. Immunol. 11, 936–944.

Selbach, M., Schwanhausser, B., Thierfelder, N., Fang, Z., Khanin, R., Rajewsky, N., 2008. Widespread changes in protein synthesis induced by microRNAs. Nature 455, 58–63.

Shouval, D.S., Biswas, A., Goettel, J.A., McCann, K., Conaway, E., Redhu, N.S., Mascanfroni, I.D., Al Adham, Z., Lavoie, S., Ibourk, M., et al., 2014. Interleukin-10 receptor signaling in innate immune cells regulates mucosal immune tolerance and anti-inflammatory macrophage function. Immunity 40, 706–719.

Spencer, S.D., Di Marco, F., Hooley, J., Pitts-Meek, S., Bauer, M., Ryan, A.M., Sordat, B., Gibbs, V.C., Aguet, M., 1998. The orphan receptor CRF2-4 is an essential subunit of the interleukin 10 receptor. J. Exp. Med. 187, 571–578.

Sun, X., Icli, B., Wara, A.K., Belkin, N., He, S., Kobzik, L., Hunninghake, G.M., Vera, M.P., Registry, M., Blackwell, T.S., et al., 2012. MicroRNA-181b regulates NF-kappaB-mediated vascular inflammation. J. Clin. Invest. 122, 1973–1990.

Tan, J.C., Indelicato, S.R., Narula, S.K., Zavodny, P.J., Chou, C.C., 1993. Characterization of interleukin-10 receptors on human and mouse cells. J. Biol. Chem. 268, 21053–21059.

Tomita, T., Kanai, T., Totsuka, T., Nemoto, Y., Okamoto, R., Tsuchiya, K., Sakamoto, N., Ohteki, T., Hibi, T., Watanabe, M., Oct 2009. IL-7 is essential for lymphopenia-driven turnover of colitogenic CD4(+) memory T cells in chronic colitis. Eur. J. Immunol. 39 (10):2737–2747. http://dx.doi.org/10.1002/eji.200838905.

Tugal, D., Liao, X., Jain, M.K., 2013. Transcriptional control of macrophage polarization. Arterioscler. Thromb. Vasc. Biol. 33, 1135–1144.

Veenbergen, S., Samsom, J.N., 2012. Maintenance of small intestinal and colonic tolerance by IL-10-producing regulatory T cell subsets. Curr. Opin. Immunol. 24, 269–276.

Weber-Nordt, R.M., Riley, J.K., Greenlund, A.C., Moore, K.W., Darnell, J.E., Schreiber, R.D., 1996. Stat3 recruitment by two distinct ligand-induced, tyrosine-phosphorylated docking sites in the interleukin-10 receptor intracellular domain. J. Biol. Chem. 271, 27954–27961.

Wehinger, J., Gouilleux, F., Groner, B., Finke, J., Mertelsmann, R., Weber-Nordt, R.M., 1996. IL-10 induces DNA binding activity of three STAT proteins (Stat1, Stat3, and Stat5)

and their distinct combinatorial assembly in the promoters of selected genes. FEBS Lett. 394, 365–370.

Zhou, L., Nazarian, A.A., Smale, S.T., 2004. Interleukin-10 inhibits interleukin-12 p40 gene transcription by targeting a late event in the activation pathway. Mol. Cell. Biol. 24, 2385–2396.

Zielinski, C.E., Mele, F., Aschenbrenner, D., Jarrossay, D., Ronchi, F., Gattorno, M., Monticelli, S., Lanzavecchia, A., Sallusto, F., 2012. Pathogen-induced human TH17 cells produce IFN-gamma or IL-10 and are regulated by IL-1beta. Nature 484, 514–518.

Zigmond, E., Bernshtein, B., Friedlander, G., Walker, C.R., Yona, S., Kim, K.W., Brenner, O., Krauthgamer, R., Varol, C., Muller, W., et al., 2014. Macrophage-restricted interleukin-10 receptor deficiency, but not IL-10 deficiency, causes severe spontaneous colitis. Immunity 40, 720–733.